

Accumulation of ionic liquids in *Escherichia coli* cells

Robert J. Cornmell,^a Catherine L. Winder,^b Gordon J. T. Tiddy,^a Royston Goodacre^b and Gill Stephens^{*a}

Received 28th April 2008, Accepted 11th June 2008

First published as an Advance Article on the web 4th July 2008

DOI: 10.1039/b807214k

Ionic liquids accumulate within *Escherichia coli* cells and can be detected by Fourier transform infrared (FT-IR) spectroscopy. Harvested cells were incubated with the biocompatible, water-immiscible ionic liquids, trihexyltetradecylphosphonium bis(trifluoromethylsulfonyl)imide ($[P_{6,6,6,14}][NTf_2]$) and methyltrioctylammonium bis(trifluoromethylsulfonyl)imide ($[N_{1,8,8,8}][NTf_2]$), and with the toxic chlorides, $[P_{6,6,6,14}][Cl]$ and $[N_{1,8,8,8}][Cl]$. The cells were harvested, washed and dried, and their FT-IR spectra were recorded. The ionic liquid spectra could be detected against the background spectra of the cells, demonstrating that they were accumulating within the cells. The toxic ionic liquids accumulated more rapidly than the biocompatible ionic liquids. Principal components analysis followed by discriminant function analysis showed that, compared to control cells, the toxic ionic liquids produced much bigger changes in the FT-IR fingerprint of the cellular chemicals than the biocompatible ionic liquids. Subcellular fractionation, followed by FT-IR analysis, demonstrated that $[P_{6,6,6,14}][NTf_2]$ accumulated specifically in the membrane fraction of the cells and not the cytoplasm.

Introduction

Ionic liquids are attracting an enormous amount of attention as clean, green alternatives to environmentally damaging conventional solvents in chemical and biocatalytic manufacturing processes.^{1–6} The most exciting feature is the unparalleled scope to tailor the solvent properties to match the requirements of the process, simply by selecting appropriate cation and anion combinations. However, this very diversity greatly complicates the task of understanding the safety and environmental impact of ionic liquids, which is crucial to obtain regulatory approval for ionic liquid-based processes and products. Fortunately, there has been remarkably rapid progress in developing structure–activity relationships for ionic liquid toxicity and environmental impact.^{7–9} However, we still know very little about the specific molecular interactions between these novel chemical entities and living organisms. For this reason, we used transmission Fourier transform infrared (FT-IR) spectroscopy to analyse the chemical composition of *Escherichia coli* cells after exposure to ionic liquids, to provide an insight into the mechanisms of toxicity.

The FT-IR spectra of cells provide metabolic fingerprints which are extremely useful for identification of microorganisms^{10–12} or to monitor their physiological state,¹³ but their use to identify naturally-occurring intracellular metabolites is generally difficult and needs complex chemometric processing.^{14–16} However, ionic liquids are xenobiotics which give

distinctive IR spectra that differ markedly from the spectra of cell components. This suggested that ionic liquids may be detectable if they accumulate inside the cells.

We tested this hypothesis by comparing the effects of toxic and biocompatible ionic liquids on the FT-IR spectra of *E. coli* cells. We chose trihexyltetradecylphosphonium bis(trifluoromethylsulfonyl)imide ($[P_{6,6,6,14}][NTf_2]$) and methyltrioctylammonium bis(trifluoromethylsulfonyl)imide ($[N_{1,8,8,8}][NTf_2]$) as examples of biocompatible ionic liquids, since they cause only modest inhibition of growth of *E. coli*.^{17,18} Furthermore, these two ionic liquids are extremely useful, since they are water-immiscible, and both can be used to provide dramatically improved product yields for redox biotransformations using bacterial cells.^{18,19} By contrast, changing the anion to chloride makes the ionic liquids so toxic that growth is inhibited completely even when the phase ratio of $[P_{6,6,6,14}][Cl]$ and $[N_{1,8,8,8}][Cl]$ is decreased to 0.0025.¹⁸ Therefore, these two ionic liquids were selected as examples of toxic, water-immiscible ionic liquids.

In this study, we show that ionic liquids are taken up into *E. coli* cells and can be readily detected against the background FT-IR spectrum of cellular chemicals. We also show that ionic liquids accumulate specifically within the membrane fraction of the cells.

Results and discussion

Effect of ionic liquids on cell viability

The first step was to produce *E. coli* cells that had been exposed to ionic liquids. *E. coli* can grow in the presence of $[P_{6,6,6,14}][NTf_2]$ and $[N_{1,8,8,8}][NTf_2]$ (although there is some inhibition) but the toxic ionic liquids, $[P_{6,6,6,14}][Cl]$ and $[N_{1,8,8,8}][Cl]$, do not allow any growth.¹⁸ Therefore, we studied the effects of the ionic liquids by first growing *E. coli* without the ionic liquids, harvesting the

^aSchool of Chemical Engineering and Analytical Science, Manchester Interdisciplinary Biocentre, University of Manchester, 131 Princess Street, Manchester, UK M1 7DN.

E-mail: gill.stephens@manchester.ac.uk; Fax: +44 161 3068918; Tel: +44 161 3064377

^bSchool of Chemistry, Manchester Interdisciplinary Biocentre, University of Manchester, 131 Princess Street, Manchester, UK M1 7DN

cells aseptically and resuspending them in fresh medium. The ionic liquids (phase ratio, 0.23; 23% v/v) were then added, and the cells were incubated for 24 h. We chose this solvent : water phase ratio because it is within the range that is suitable for two-liquid phase biotransformations²⁰ and because it allows direct comparison with our previous work on biotransformations using ionic liquids.¹⁸

Using culture medium meant that there was some growth in the control cell suspensions during the first 3 h, and in the suspensions exposed to $[N_{1,8,8,8}][NTf_2]$ and $[P_{6,6,6,14}][NTf_2]$ (Fig. 1). However, there was little growth thereafter. The optical (OD) and viable count were slightly lower in the cell suspensions exposed to these ionic liquids than in the control without ionic liquid.

By contrast, $[N_{1,8,8,8}][Cl]$ and $[P_{6,6,6,14}][Cl]$ both caused a dramatic decrease in OD when added to the cell suspensions, indicating that the cells were lysing. The cells began to recover after exposure to $[P_{6,6,6,14}][Cl]$ for 3 h, and there was a slight increase in the viable count and OD after 24 h. $[N_{1,8,8,8}][Cl]$ was completely bacteriocidal, since viable cells could not be detected. Thus, no colonies were formed even when the undiluted cell suspension was spread on agar plates. Similar behaviour was observed even when the phase ratio was decreased to 0.05. Nevertheless, sufficient residual cell material could be collected for FT-IR analysis by centrifugation. We assumed that this material consisted of dead cells and cell fragments.

FTIR spectroscopy of cells exposed to $[P_{6,6,6,14}]^+$ -containing ionic liquids

Next, we measured the FT-IR spectra of the cells after exposure to the ionic liquids, and compared them with the spectra of pure ionic liquids and with unexposed control cells. Exposure to $[P_{6,6,6,14}][NTf_2]$ had very little effect on the cell spectra after 30 min or 3 h (Fig. 2). However, the spectrum was dominated by the extremely distinctive fingerprint of $[P_{6,6,6,14}][NTf_2]$ after 24 h. This demonstrated that the ionic liquid was either being taken up by the cells or was so tightly bound to the cell surface that it could not be removed by our vigorous washing procedure. The fact that there was little accumulation during the first 3 h indicates either that the accumulation process was slow or that the cells were excluding the ionic liquid. Comparison of the spectra (Fig. 2) with the spectra of cells exposed to $[P_{6,6,6,14}][Cl]$ (Fig. 3) makes it possible to distinguish the peaks due to the cation and the anion, since, of course, the Cl^- anion does not give an FTIR signal. This comparison shows that the peaks were due to both the $P_{6,6,6,14}^+$ cation and the NTf_2^- anion, indicating that both were present in the cells.

The spectra of cells exposed to the toxic ionic liquid, $[P_{6,6,6,14}][Cl]$, contained small peaks due to the ionic liquid even after 30 min (Fig. 3). Therefore, accumulation of the toxic ionic liquid began more quickly than in the samples exposed to $[P_{6,6,6,14}][NTf_2]$. The intensity of the peaks increased relative to the cell fingerprint after 3 h, but decreased again after 24 h. This suggests that the ionic liquid was lost from the cells after prolonged incubation. Whether this was due to leakage or active exclusion associated with recovery of the cells (Fig. 1) remains to be determined.

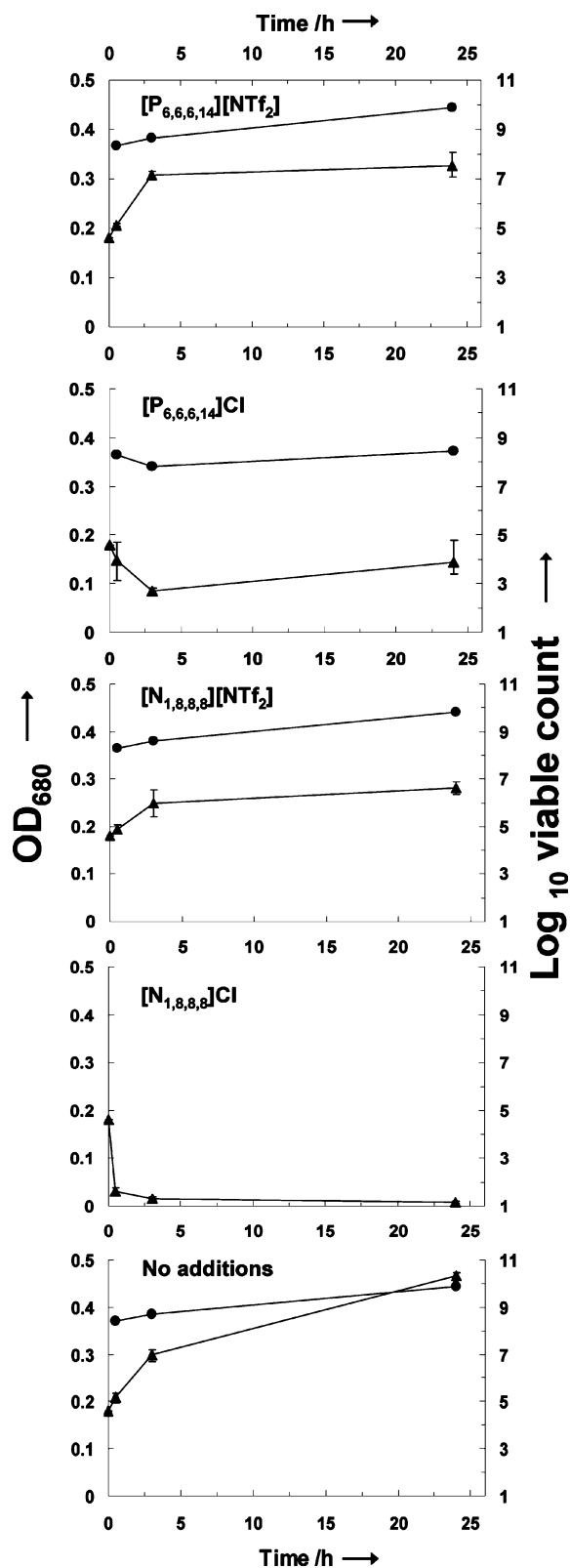


Fig. 1 Effect of ionic liquids on the optical density and viable count of *E. coli* after harvesting and resuspension in fresh culture medium. The cells were incubated with the ionic liquids shown and the OD (\blacktriangle) and viable counts (\bullet) were measured.

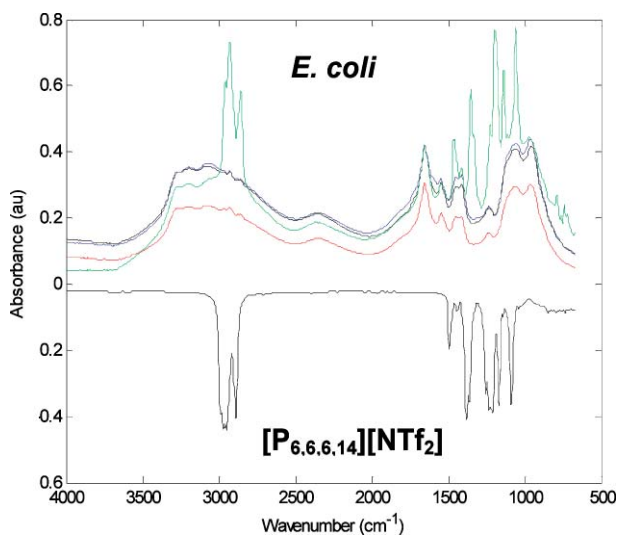


Fig. 2 FT-IR spectra of *E. coli* after exposure to $[P_{6,6,6,14}][NTf_2]$ after 30 min (green), 3 h (red) and 24 h (turquoise), or without ionic liquid (blue). The spectrum of authentic $[P_{6,6,6,14}][NTf_2]$ is plotted upside down for comparison.

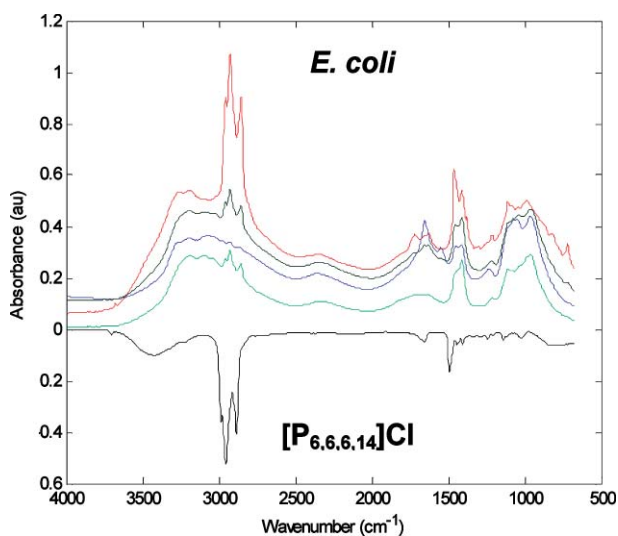


Fig. 3 FT-IR spectra of *E. coli* after exposure to $[P_{6,6,6,14}][Cl]$ after 30 min (green), 3 h (red) and 24 h (turquoise), or without ionic liquid (blue). The spectrum of authentic $[P_{6,6,6,14}][Cl]$ is plotted upside down for comparison.

FTIR spectroscopy of cells exposed to $[N_{1,8,8,8}]^+$ -containing ionic liquids

The FT-IR spectra of cells exposed to the biocompatible ionic liquid, $[N_{1,8,8,8}][NTf_2]$, contained small peaks due to the ionic liquid throughout the incubation period (Fig. 4). Comparison with spectra of cells exposed to $[N_{1,8,8,8}][Cl]$ (Fig. 5) shows that both the cation and the anion could be detected. However, it is difficult to interpret the kinetics of accumulation because the peak intensities were low, and the ratios of signal intensity between the cation and anion peaks cannot be judged accurately. Nevertheless, the fact that the ionic liquid accumulated rapidly is consistent with its increased growth inhibition compared with $[P_{6,6,6,14}][NTf_2]$.¹⁸

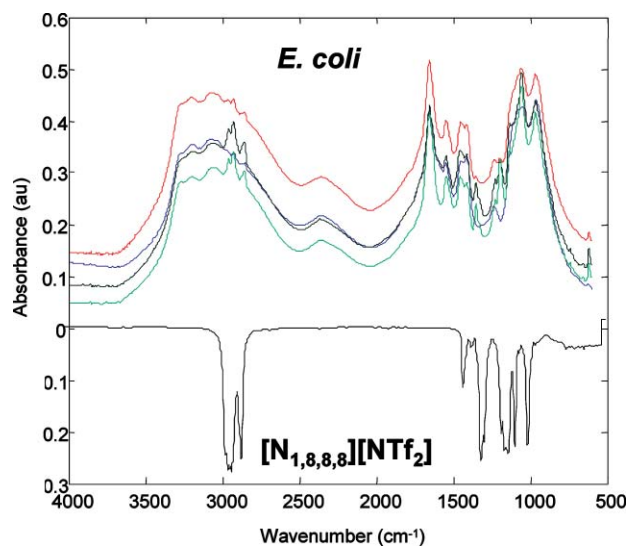


Fig. 4 FT-IR spectra of *E. coli* after exposure to $[N_{1,8,8,8}][NTf_2]$ after 30 min (green), 3 h (red) and 24 h (turquoise), or without ionic liquid (blue). The spectrum of authentic $[N_{1,8,8,8}][NTf_2]$ is plotted upside down for comparison.

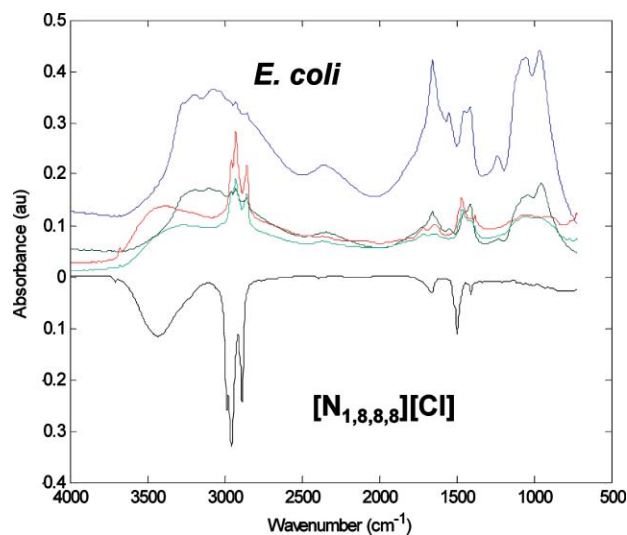


Fig. 5 FT-IR spectra of *E. coli* after exposure to $[N_{1,8,8,8}][Cl]$ after 30 min (green), 3 h (red) and 24 h (turquoise), or without ionic liquid (blue). The spectra of the cells exposed to the ionic liquid are much less intense than the control because there was extensive cell lysis, which caused loss of cell material. The spectrum of authentic $[N_{1,8,8,8}][Cl]$ is plotted upside down for comparison.

In cells exposed to $[N_{1,8,8,8}][Cl]$, the $N_{1,8,8,8}^+$ cation could be detected clearly after 3 h and 24 h, although it was not clear whether the ionic liquid was present or not after 30 min (Fig. 5). The background cell fingerprint was much weaker than in the control cells because very little cell material was available for analysis due to cell lysis (see Fig. 1). However, the peak intensities due to the ionic liquids were strong relative to the cell peaks, suggesting that the residual dead cell material had a very high capacity to bind the ionic liquid. As with $[P_{6,6,6,14}][Cl]$, $[N_{1,8,8,8}][Cl]$ accumulated in the cells relatively quickly, and this suggests that early accumulation of the ionic liquid is associated with

toxicity. However, methods for kinetic analysis would need to be developed to verify this hypothesis.

Analysis of FTIR data

Intracellular accumulation of the ionic liquids could be detected by simple visual inspection of the FT-IR spectra. However, FT-IR spectroscopy can also be used as a metabolic “fingerprinting” technique to detect changes in cell physiology.^{15,21,22} Therefore, we also wanted to find out if the spectra indicated any changes in the underlying cell chemistry. The complexity of cellular FT-IR spectra makes it essential to use multivariate statistical analysis methods to quantify the differences and identify differences between the spectra that may be attributable to the underlying biology and chemistry.^{23–25} Therefore, the multidimensional FT-IR data (1764 data points) were reduced by principal components analysis (PCA). Discriminant function analysis (DFA) was then used to discriminate between groups on the basis of the retained principal components and the *a priori* knowledge of which spectra were machine replicates.

Clustering patterns could be obtained from PC-DFA of the data with only 5 PCs selected (Fig. 6). The cell samples exposed to the biocompatible ionic liquid, [N_{1,8,8,8}][NTf₂], were located close to the tight cluster of the control cells, which had not been exposed to solvent. Therefore, [N_{1,8,8,8}][NTf₂] had relatively little effect on the metabolic fingerprint of the cells, suggesting that there was little perturbation of cellular chemistry.

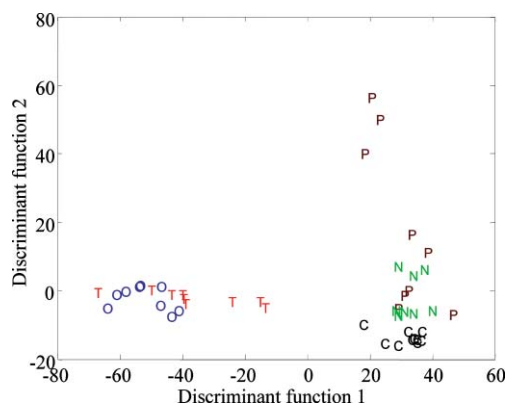


Fig. 6 PC-DFA scores plot based on the first 5 principal components from FT-IR spectra analysed by Matlab. The plot shows the relationship between FT-IR spectra of *E. coli* incubated without ionic liquids (C, black), or with [P_{6,6,6,14}][NTf₂] (P, brown), [N_{1,8,8,8}][NTf₂] (N, green), [P_{6,6,6,14}][Cl] (T, red) or [N_{1,8,8,8}][Cl] (O, blue) for 24 h.

The spectra of cells exposed to [P_{6,6,6,14}][NTf₂] clustered much less tightly with the controls, since one of the biological replicates clustered away from the controls in the second discriminant function (DF). However, it should be noted that the peaks due to [P_{6,6,6,14}][NTf₂] were very intense (see Fig. 2) and tended to dominate the underlying cell fingerprint, and this may have caused this change.

By contrast, the spectra of cells exposed to the toxic ionic liquids, [P_{6,6,6,14}][Cl] and [N_{1,8,8,8}][Cl] formed clusters that were completely distinct from the control cluster and were clearly separated from the controls and biocompatible ionic liquids in the first DF. This is highly significant because the first DF

is extracted to give the most variance with respect to group separation. The facts that the DFA algorithm was trained with machine replicates and not the toxicity (or otherwise) of the ionic liquid, and that the differentiation between toxic *versus* benign ionic liquids occurs in the first DF show that there are clear phenotypic differences between the *E. coli* cells when they are exposed to toxic ionic liquids compared to the controls and cells exposed to non-toxic solvents. Moreover, these ionic liquids should have a weaker influence on the overall spectrum than the bis-triflamide-containing ionic liquids, since we could see only the cation spectra superimposed on the underlying cell spectra. Therefore, the extent of the separation from the controls observed in Fig. 6 suggests further that the toxic ionic liquids really do have a marked effect on cellular biochemistry. Detailed metabolomic analysis will be needed in the future to identify the specific biochemical changes that were induced by the toxic ionic liquids.

FTIR spectroscopy of subcellular fractions

We were extremely curious to find out where the ionic liquids were accumulating in the cells. Therefore, we grew *E. coli* in the presence of [P_{6,6,6,14}][NTf₂], harvested the cells and fractionated them into cytoplasmic and membrane fractions. We also collected the residual buffer from the washing step, to check for leakage of the ionic liquids. We then measured the FT-IR spectra of the subcellular fractions and compared them with fractions from cells that had not been exposed to the ionic liquid (Fig. 7). Remarkably, the ionic liquid could only be detected in the cell membranes, and not in the cytoplasmic fraction or the extracellular wash fraction. Therefore, it seems that this hydrophobic ionic liquid is lipophilic enough to accumulate in the membranes, even though it causes relatively little growth inhibition.

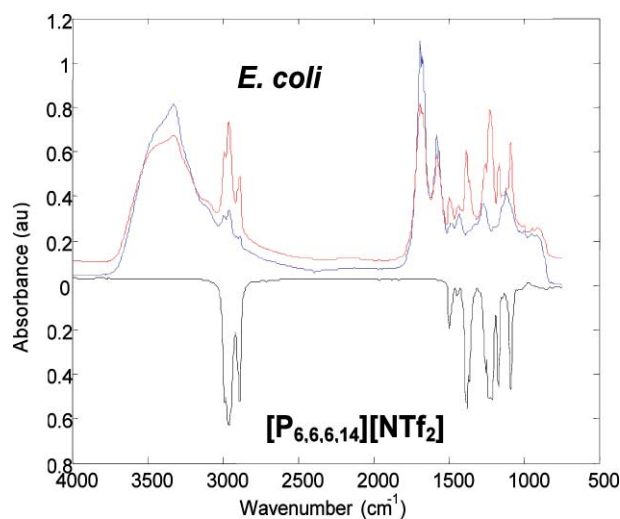


Fig. 7 FT-IR spectra of membrane fractions (red) of *E. coli* after growth in the presence of [P_{6,6,6,14}][NTf₂], compared with membrane fractions from unexposed cells (blue). For clarity, the spectra of cytoplasmic and wash fractions are not shown, since the ionic liquid could not be detected in either. The spectrum of authentic [P_{6,6,6,14}][NTf₂] is plotted upside down for comparison.

Conclusions

We have shown that FT-IR spectroscopy can be used to detect accumulation of ionic liquids inside microbial cells, and that there may be a connection between speed of accumulation and toxicity. FT-IR spectroscopy is especially convenient to use to study intracellular uptake because the ionic liquids can be detected without having to label them with heavy isotopes or radiolabels. Furthermore, FT-IR analysis can be applied to a wide range of cell types^{10,12,26,27} and can be done conveniently and rapidly in 96 well format.^{11,28} This makes FT-IR very attractive for high throughput screening for ionic liquid uptake.

The detection of ionic liquids inside cells provides an important advance in understanding the mechanisms of ionic liquid toxicity. The direct demonstration that ionic liquids really do partition into lipid membranes in cells is especially significant. There is a growing body of evidence that the toxicity of ionic liquids is strongly correlated with their lipophilicity,^{7,29–32} suggesting that toxicity is due to disruption of membrane structure. Our findings provide excellent mechanistic support for this correlation.

In conclusion, this is the first use of FT-IR spectroscopy to demonstrate the accumulation of ionic liquids within bacterial cells and their membranes, and provides a very sound basis for further, detailed investigation of toxicity mechanisms.

Experimental

Chemicals

[N_{1,8,8,8}][NTf₂], were purchased from Solvent Innovation, and [N_{1,8,8,8}][Cl], [P_{6,6,6,14}][Cl] and [P_{6,6,6,14}][NTf₂] were obtained from Sigma–Aldrich. All other reagents and media components were purchased from Sigma–Aldrich, unless otherwise stated.

Exposure of harvested cells to ionic liquids

Escherichia coli K12 MG1655³³ was maintained on LB agar. Inocula and experimental cultures were grown in MSX medium³⁴ at 37 °C with shaking at 200 rpm. Experimental cultures (150 ml; 1% inoculum) were grown for 24 h, divided into 15 separate aliquots (10 ml) and harvested by centrifugation at 4000 rpm for 10 min at 4 °C. The cell pellets were resuspended in 10 ml MSX medium as a control or 7.7 ml MSX medium plus 2.3 ml of ionic liquid, with 3 replicates for each condition. After incubation at 37 °C with shaking at 200 rpm, samples of the aqueous phases of the cultures were taken for measurement of OD₆₈₀, viable count measurements and FT-IR analysis. Viable counts were measured by serially diluting the samples in physiological saline (0.9% NaCl) and plating 100 µl aliquots on LB agar.

Sample preparation

Cells were prepared for FTIR analysis by taking samples of the aqueous phases of the cell suspensions during exposure to ionic liquids (2 ml). The cells were collected by centrifugation at 13 000 rpm for 3 min, washed 3 times by vortex mixing in physiological saline (1 ml) and resuspended in saline to give the same approximate cell concentration as the control sample. Thus, the control cells, and cells exposed to [P_{6,6,6,14}][NTf₂] and

[N_{1,8,8,8}][NTf₂] were resuspended in 125 µl saline, and samples exposed to [P_{6,6,6,14}][Cl] were resuspended in 62 µl saline. The cell concentration in samples exposed to [N_{1,8,8,8}][Cl] was extremely low, and so the samples were resuspended in 25 µl saline, the minimum possible volume suitable for analysis.

Subcellular fractionation

Cultures (50 ml) of *E. coli* were grown for 24 h at 37 °C in the presence of [P_{6,6,6,14}][NTf₂] (phase ratio 0.23) in MSX medium. The cells were harvested from the aqueous phase by centrifugation at 4000 rpm for 20 min at 4 °C. The resulting pellet was washed twice by resuspension in saline (5 ml), and harvested as before. The supernatants from both washing steps were pooled and stored for FT-IR analysis. The final cell pellet was resuspended in saline (2 ml) and disrupted using a homogeniser (Kinematica) for 10 min on ice. The homogenate was filtered through a 0.2 µm filter to remove any unbroken cells and cell wall debris, and then centrifuged at 13 000 rpm for 1 h at 4 °C. The pellet (cell membrane fraction) was resuspended in 200 µl saline. The membranes and the supernatant (cytoplasmic fraction) were then analysed immediately by FT-IR.

FT-IR spectroscopy

The cell samples were analysed in triplicate as detailed elsewhere.^{11,12,26} Aliquots (25 µl) of cell suspensions were applied evenly onto a zinc selenide (Bruker) plate for analysis by FT-IR. The samples were dried at 50 °C for 30 min. The plate was loaded onto a motorised microplate module HTS-XTTM attached to an Equinox 55 module (Bruker Optics Ltd., UK). A deuterated triglycine sulfate (DTGS) detector was employed for transmission measurements of the samples. Spectra were collected over the wavelength range of 4000 to 900 cm⁻¹ under the control of a computer programmed with Opus 4, operated under MS windows 2000. Spectra were acquired at a resolution of 4 cm⁻¹ and 64 spectra were co-added and averaged to improve the signal to noise ratio. The collection time for each spectrum was approximately 1 min, and the spectra were displayed in terms of absorbance. It should be noted that the FTIR spectra contain smaller peaks due to lipid and larger peaks due to polysaccharide than normally found in growing cells because the cells were not growing actively during the experiments. Authentic FT-IR spectra from [P_{6,6,6,14}][NTf₂], [P_{6,6,6,14}][Cl], [N_{1,8,8,8}][Cl] and [N_{1,8,8,8}][NTf₂] were acquired by loading 0.8 µl aliquots of each ionic liquid onto a calcium fluoride disc and collecting spectra from a mercury cadmium telluride (MCT) detector after initial measurement with a 15× objective lens.

Cluster analysis

Analysis of the FT-IR data was based on methods described previously.^{11,12,26} The multidimensional FT-IR data were reduced by principal components analysis (PCA).³⁵ PCA was performed according to the NIPALS algorithm.³⁶ In this manner the multivariate FT-IR spectra (containing 1764 data points) were reduced down to 5 PCs and discriminant function analysis (DFA) then discriminated between groups on the basis of the retained principal components and the *a priori* knowledge of which spectra were machine replicates (so for each of the

3 biological replicates which were analysed 3 times, 3 classes were used for each ionic liquid by the DFA algorithm). Thus, this process did not bias the analysis in any way.³⁷ These cluster analysis methods were implemented using Matlab version 7.1 (The Math Works, Inc., Natick, MA, USA), which runs under Microsoft Windows NT.

Acknowledgements

We are grateful to the Engineering and Biological Systems committee of the UK Biotechnology and Biological Sciences Research Council for financial support *via* grant number BB/C503346/1

References

- 1 M. Deetlefs and K. R. Seddon, *Chim. Oggi*, 2006, **24**, 16–23.
- 2 N. V. Plechkova and K. R. Seddon, *Chem. Soc. Rev.*, 2008, **37**, 123–150.
- 3 F. van Rantwijk, R. Madeira Lau and R. A. Sheldon, *Trends Biotechnol.*, 2003, **21**, 131–138.
- 4 S. Park and R. J. Kazlauskas, *Curr. Opin. Biotechnol.*, 2003, **14**, 432–437.
- 5 S. Cantone, U. Hanefeld and A. Basso, *Green Chem.*, 2007, **9**, 954–971.
- 6 F. Van Rantwijk and R. A. Sheldon, *Chem. Rev.*, 2007, **107**, 2757–2785.
- 7 J. Ranke, S. Stolte, R. Stoermann, J. Arning and B. Jastorff, *Chem. Rev.*, 2007, **107**, 2183–2206.
- 8 B. Jastorff, K. Moelter, P. Behrend, U. Bottin-Weber, J. Filser, A. Heimers, B. Ondruschka, J. Ranke, M. Schaefer, H. Schroeder, A. Stark, P. Stepnowski, F. Stock, R. Stoermann, S. Stolte, U. Welz-Biermann, S. Ziegert and J. Thoeming, *Green Chem.*, 2005, **7**, 362–372.
- 9 B. Jastorff, R. Stoermann, J. Ranke, K. Moelter, F. Stock, B. Oberheitmann, W. Hoffmann, J. Hoffmann, M. Nuechter, B. Ondruschka and J. Filser, *Green Chem.*, 2003, **5**, 136–142.
- 10 K. Maquelin, C. Kirschner, L. P. Choo-Smith, N. Van Den Braak, H. P. Endtz, D. Naumann and G. J. Puppels, *J. Microbiol. Methods*, 2002, **51**, 255–271.
- 11 C. L. Winder, S. V. Gordon, J. Dale, R. G. Hewinson and R. Goodacre, *Microbiology*, 2006, **152**, 2757–2765.
- 12 E. M. Timmins, S. A. Howell, B. K. Alsberg, W. C. Noble and R. Goodacre, *J. Clin. Microbiol.*, 1998, **36**, 367–374.
- 13 H. E. Johnson, D. Broadhurst, D. B. Kell, M. K. Theodorou, R. J. Merry and G. W. Griffith, *Appl. Environ. Microbiol.*, 2004, **70**, 1583–1592.
- 14 R. Goodacre, B. Shann, R. J. Gilbert, É. M. Timmins, A. C. McGovern, B. K. Alsberg, D. B. Kell and N. A. Logan, *Anal. Chem.*, 2000, **72**, 119–127.
- 15 W. B. Dunn, N. J. C. Bailey and H. E. Johnson, *Analyst*, 2005, **130**, 606–625.
- 16 A. C. McGovern, D. Broadhurst, J. Taylor, N. Kaderbhai, M. K. Winson, D. A. Small, J. J. Rowland, D. B. Kell and R. Goodacre, *Biotechnol. Bioeng.*, 2002, **78**, 527–538.
- 17 H. Pfruender, R. Jones and D. Weuster-Botz, *J. Biotechnol.*, 2006, **124**, 182–190.
- 18 R. J. Cormell, C. L. Winder, S. Schuler, R. Goodacre and G. Stephens, *Green Chem.*, 2008, **10**, 685–691.
- 19 H. Pfruender, M. Midjojo, U. Kragl and D. Weuster-Botz, *Angew. Chem., Int. Ed.*, 2004, **43**, 4529–4531.
- 20 R. Leon, P. Fernandes, H. M. Pinheiro and J. M. S. Cabral, *Enzyme Microb. Technol.*, 1998, **23**, 483–500.
- 21 D. I. Ellis and R. Goodacre, *Analyst*, 2006, **131**, 875–885.
- 22 K. Hollywood, D. R. Brison and R. Goodacre, *Proteomics*, 2006, **6**, 4716–4723.
- 23 R. Goodacre, *J. Exp. Bot.*, 2005, **56**, 245–254.
- 24 R. Goodacre, S. Vaidyanathan, W. B. Dunn, G. G. Harrigan and D. B. Kell, *Trends Biotechnol.*, 2004, **22**, 245–252.
- 25 R. M. Jarvis and R. Goodacre, *Bioinformatics*, 2005, **21**, 860–868.
- 26 R. Goodacre, É. M. Timmins, R. Burton, N. Kaderbhai, A. M. Woodward, D. B. Kell and P. J. Rooney, *Microbiology*, 1998, **144**, 1157–1170.
- 27 D. Naumann, D. Helm and H. Labischinski, *Nature*, 1991, **351**, 81–82.
- 28 G. G. Harrigan, R. H. LaPlante, G. N. Cosma, G. Cockerell, R. Goodacre, J. F. Maddox, J. P. Luyendyk, P. E. Ganey and R. A. Roth, *Toxicol. Lett.*, 2004, **146**, 197–205.
- 29 J. Ranke, K. Molter, F. Stock, U. Bottin-Weber, J. Poczbott, J. Hoffmann, B. Ondruschka, J. Filser and B. Jastorff, *Ecotoxicol. Environ. Saf.*, 2004, **58**, 396–404.
- 30 S. Stolte, M. Matzke, J. Arning, A. Boeschen, W.-R. Pitner, U. Welz-Biermann, B. Jastorff and J. Ranke, *Green Chem.*, 2007, **9**, 1170–1179.
- 31 J. Ranke, A. Mueller, U. Bottin-Weber, F. Stock, S. Stolte, J. Arning, R. Stoermann and B. Jastorff, *Ecotoxicol. Environ. Saf.*, 2007, **67**, 430–438.
- 32 J. Ranke, K. Moelter, F. Stock, U. Bottin-Weber, J. Poczbott, J. Hoffmann, B. Ondruschka, J. Filser and B. Jastorff, *Ecotoxicol. Environ. Saf.*, 2004, **58**, 396–404.
- 33 F. R. Blattner, G. Plunkett, C. A. Bloch, N. T. Perna, V. Burland, M. Riley, J. ColladoVides, J. D. Glasner, C. K. Rode, G. F. Mayhew, J. Gregor, N. W. Davis, H. A. Kirkpatrick, M. A. Goeden, D. J. Rose, B. Mau and Y. Shao, *Science*, 1997, **277**, 1453–1462.
- 34 L. P. Wahbi, D. Gokhale, S. Minter and G. M. Stephens, *Enzyme Microb. Technol.*, 1996, **19**, 297–306.
- 35 I. T. Jolliffe, *Principal Component Analysis*, Springer-Verlag, New York, 1986.
- 36 H. Wold, in *Multivariate Analysis*, ed. K. R. Krishnaiah, Academic Press, New York, 1966, pp. 391–420.
- 37 B. F. J. Manly, *Multivariate Statistical Methods: A Primer*, Chapman & Hall, London, 1994.